Characterization of *Mycobacterium tuberculosis* Mycothiol *S*-Conjugate Amidase†

Micah Steffek,‡ Gerald L. Newton,‡ Yossef Av-Gay,§ and Robert C. Fahey*,‡

Department of Chemistry and Biochemistry, University of California at San Diego, La Jolla, California 92093, and Department of Medicine, University of British Columbia, Vancouver, BC V5Z 3J5, Canada

Received April 2, 2003; Revised Manuscript Received July 21, 2003

ABSTRACT: Mycothiol is comprised of *N*-acetylcysteine (AcCys) amide linked to 1D-*myo*-inosityl 2-amino-2-deoxy-α-D-glucopyranoside (GlcN-Ins) and is the predominant thiol found in most actinomycetes. Mycothiol *S*-conjugate amidase (Mca) cleaves the amide bond of mycothiol *S*-conjugates of a variety of alkylating agents and xenobiotics, producing GlcN-Ins and a mercapturic acid that can be excreted from the cell. Mca of *Mycobacterium tuberculosis* (Rv1082) was cloned and expressed as a soluble protein in *Escherichia coli*. The protein contained 1.4 ± 0.1 equiv of zinc after purification, indicating that Mca is a metalloprotein with zinc as the native metal. Kinetic studies of Mca activity with 14 substrates demonstrated that Mca is highly specific for the mycothiol moiety of mycothiol *S*-conjugates and relatively nonspecific for the structure of the sulfur-linked conjugate. The deacetylase activity of Mca with GlcNAc-Ins is small but significant and failed to saturate at up to 2 mM GlcNAc-Ins, indicating that Mca may contribute modestly to the production of GlcN-Ins when GlcNAc-Ins levels are high. The versatility of Mca can be seen in its ability to react with a broad range of mycothiol *S*-conjugates, including two different classes of antibiotics. The mycothiol *S*-conjugate of rifamycin S was produced under physiologically relevant conditions and was shown to be a substrate for Mca in both oxidized and reduced forms. Significant activity was also seen with the mycothiol *S*-conjugate of the antibiotic cerulenin as a substrate for Mca.

Mycothiol [MSH,[1] AcCys-GlcN-Ins, 1D-*myo*-inosityl 2-(*N*-acetylcysteinyl)amido-2-deoxy-α-D-glucopyranoside] is the primary low-molecular weight thiol in most actinomycetes and is present at especially high levels in mycobacteria (*1*). Like glutathione, mycothiol is maintained in a reduced state by mycothiol disulfide reductase and appears to play a key role in protecting the cell against oxidative stress and challenge by electrophilic toxins (*2*−*4*). Mycothiol plays a role in the detoxification of formaldehyde (*5*−*7*) and nitric oxide (*8*), in the neutralization of alkylating agents (*9*), and in the metabolism of certain antibiotics (*10*, *11*).

A key enzyme involved in MSH-dependent detoxification is mycothiol *S*-conjugate amidase (Mca), first isolated from *Mycobacterium smegmatis* (*9*). Mycothiol *S*-conjugate amidase hydrolyzes the cysteinyl−glucosamine amide bond of the mycothiol *S*-conjugate (MSR), releasing the AcCys *S*-conjugate (a mercapturic acid), which can be excreted into the medium, and the GlcN-Ins moiety, which is retained in the cell and used for the regeneration of mycothiol (Scheme 1). Mercapturic acid production is a major detoxification pathway in mammals, but the source of the cysteine in the mercapturic acid pathway is GSH (*12*). The pathway in mammals utilizes at least four enzymes from various tissues and several transport systems. In contrast, formation of the mycothiol *S*-conjugate in mycobacteria is followed immediately by Mca-promoted cleavage which releases the mercapturic acid (*9*).

Although the natural substrates of the mycothiol *S*-conjugate amidase are not known, the *S*-conjugate of the tuberculosis drug cerulenin has been shown to be a substrate of Mca (*9*). Searching structural databases (SciFinder Scholar, Chemical Abstracts Service, Columbus, OH) reveals that the majority of naturally occurring mercapturic acids are found in either mammals or actinomycetes (*4*). Homologues of Mca have been reported in the antibiotic biosynthetic operons of other actinomycetes (*4*), the majority of which produce mycothiol (*1*). This, combined with the finding of mercapturic acids in the fermentation broths of streptomycetes, has led to the proposal that Mca is used to detoxify antibiotics

† The research of R.C.F. was supported by the National Institute of Allergy and Infectious Diseases (Grant AI49174) and by eXegenics Corp., and that of Y.A. was supported by the TB Veterans Association. Y.A. is a British Columbia Lung Association−Canadian Institute of Health Research Scholar.

* To whom correspondence should be addressed. Phone: (858) 534-2163. Fax: (858) 534-4864. E-mail: rcfahey@ucsd.edu.

‡ University of California, San Diego.

§ University of British Columbia.

[1] Abbreviations: AccQ-fluor, 6-aminoquinolyl-*N*-hydroxysuccinimidyl carbamate; AcCys, *N*-acetylcysteine; AcCys-GlcN, 2-(*N*-acetyl-L-cysteinyl)amido-2-deoxy-(α,β)-D-glucopyranoside; CPM, 7-(diethylamino)-3-(4′-maleimidylphenyl)-4-methylcoumarin; Cys-GlcN-Ins, 1D-*myo*-inosityl 2-(L-cysteinyl)amido-2-deoxy-α-D-glucopyranoside; GlcN-Ins, 1D-*myo*-inosityl 2-amino-2-deoxy-α-D-glucopyranoside; HEPES, *N*-(2-hydroxyethyl)piperazine-*N*′-2-ethanesulfonic acid; HPLC, high-performance liquid chromatography; MALDI-FTMS, matrix-assisted laser desorption and ionization-Fourier transform mass spectroscopy; mBBr, monobromobimane; Mca, mycothiol *S*-conjugate amidase; MPB, 3-(*N*-maleimidopropionyl)biocytin; MS−acetamide, iodoacetamide *S*-conjugate of mycothiol; MSC, cerulenin *S*-conjugate of mycothiol; MSH, mycothiol, 1D-*myo*-inosityl 2-(*N*-acetylcysteinyl)amido-2-deoxy-α-D-glucopyranoside; MSME, NEM *S*-conjugate of mycothiol; MSMC, CPM *S*-conjugate of mycothiol; MSMPB, MPB *S*-conjugate of mycothiol; NEM, *N*-ethylmaleimide; ORF, open reading frame; PAGE, polyacrylamide gel electrophoresis; RifS, rifamycin S; RifS13, reduced mycothiol *S*-conjugate of rifamycin S; RifS17, oxidized mycothiol *S*-conjugate of rifamycin S; RSmB, bimane derivative of corresponding thiol RSH; SDS, sodium dodecyl sulfate; Tris, tris(hydroxymethyl)-aminomethane.

10.1021/bi030080u CCC: $25.00
Published on Web 09/27/2003

Scheme 1: Hydrolysis of Mycothiol *S*-Conjugates (MSR) by Mca

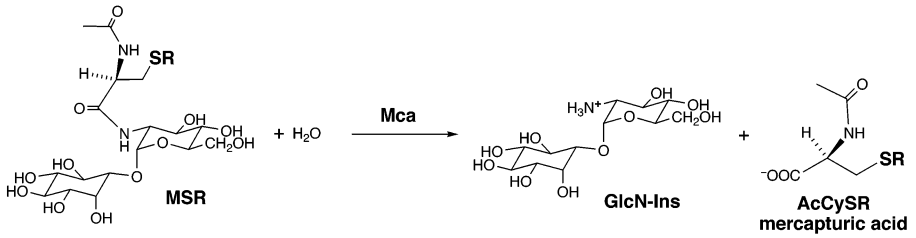

and electrophilic drugs in actinomycetes (*4*). Recently, inhibitors of Mca have been found in natural product and synthetic libraries, and these provide potential lead compounds for the development of drugs directed against the Mca target (*13*−*15*). Mycothiol and Mca are not found in GSH-producing mammals, so drugs inhibiting Mca may be less toxic than those for other drug targets. Thus, Mca may be an attractive new target for drugs directed against drug resistant tuberculosis (*16*).

In the study presented here, the *mca* gene of *Mycobacterium tuberculosis* (Rv1082) was cloned and expressed in *Escherichia coli* as the native protein and purified to homogeneity. The enzyme was characterized in terms of its metal ion requirement and its substrate specificity. Products of the reaction of rifamycin S with mycothiol were identified and shown to be substrates for Mca.

MATERIALS AND METHODS

Reagents. MSH was isolated from *M. smegmatis* and was purified along with its oxidized form (MSSM) by preparative HPLC as described previously (*17*). *N*-Formyl-CySmB-GlcN-Ins (previously designated U18) and CySmB-GlcN-Ins were isolated by preparative HPLC, using a protocol similar to that described elsewhere (*18*), from a monobromobimane (mBBr, Molecular Probes)-derivatized 50% acetonitrile extract of a 26 g wet weight pellet of late exponential cells of *M. smegmatis* strain *mshD*:Tn*5* (*19*). GlcNAc-Ins was prepared from the bimane derivative of MSH (MSmB) by enzymatic cleavage with Mca and acetylation as previously described (*20*). The bimane derivative (AcCySmB-GlcN) of 1-(*N*-acetylcysteinyl)amido-2-deoxy-α-D-glucopyranose (AcCys-GlcN) (*17*) was prepared by derivatization with mBBr according to the method for production of standards (*21*). Rifamycin S was kindly provided by R. M. Vohra (Institute of Microbial Technology, Sector 39A, Chandigarh 160036, India). The sodium salt of rifamycin SV was purchased from Sigma. Unless otherwise specified, other reagent chemicals were purchased from Fisher and were ACS grade or the highest purity offered. All growth media were purchased from Difco (Becton Dickenson).

Mycothiol S-Conjugates. Mycothiol *S*-conjugates other than MSmB were prepared by reaction of excess electrophile with mycothiol followed by preparative HPLC purification. Reaction of cerulenin (Sigma, 110 mM stock in methanol) and *N*-ethylmaleimide (Sigma, 310 mM stock in methanol) at 35 mM in 150 mM HEPES chloride (pH 7.5) was initiated by the addition of mycothiol to a final concentration of 30 mM from a 107 mM stock solution in H_2O (pH ∼3) and was allowed to proceed for 2 h in the dark. Reactions with 7-(diethylamino)-3-(4′-maleimidylphenyl)-4-methylcoumarin (CPM, Molecular Probes, 50 mM stock in methanol) and 3-(*N*-maleimidopropionyl)biocytin (MPB, Molecular Probes, 50 mM in dimethyl sulfoxide) at 20 mM in 150 mM HEPES chloride (pH 7.5) were initiated by the addition of mycothiol to a final concentration of 10 mM from a 107 mM stock solution in H_2O (pH ∼3) and were allowed to proceed for 2 h in the dark. The mycothiol adducts (MS−cerulenin, MS−CPM, MS−MPB, and MS−ME) were isolated by preparative HPLC on a Beckman Ultrasphere IP (250 mm × 4.6 mm) analytical column equipped with a C-18 HPLC guard column using the following elution protocol: 100% A (water, pH unadjusted) from 0 to 5 min, a linear gradient to 40% B (acetonitrile for the MS−CPM and MS−ME conjugates or methanol for the MS−cerulenin and MS−MPB conjugates) from 5 to 40 min, 100% B at 45 min, and returning to 100% A at 50 min with reinjection at 60 min. The flow rate was 1 mL/min, and the effluent was monitored by the absorbance at 220 nm (Waters 486). The mycothiol adducts were taken to 10% of the collected volume in a Savant Sped-Vac and brought back to the desired concentration in water. The MSH adduct of acetophenone (MS−acetophenone) was prepared by reaction of 13 mM bromoacetophenone (Acros) with 10 mM MSH in 50% acetonitrile containing 25 mM Tris (pH 8) for 30 min at 22 °C. The residual level of thiol was less than 2% by titration with 5,5′-dithiobis(2-nitrobenzoic acid) (Sigma). The conjugate was purified by HPLC on a 22 mm × 250 mm Beckman Ultrasphere ODS IP column. The mycothiol *S*-conjugates of RifS13 and RifS17 are described below.

The mycothiol *S*-conjugate stock solutions were calibrated by determination of the amount of GlcN-Ins released upon treatment with purified Mca. Reaction of ∼500 pmol of *S*-conjugate in 50 μL of 50 mM HEPES (pH 7.5) containing 50 mM NaCl and 0.1 mM DTT was initiated by addition of 3 μg of purified Mca. The reaction mixture was sampled (10 μL) at 30, 60, 90, and 120 min, and an additional 1.4 μg of Mca was added at the first three time points. The reactions were quenched by mixing with an equal volume of acetonitrile containing 10 mM NEM (Sigma) and 2 mM 1,10-phenanthroline (Kodak) followed by incubation at 60 °C for 10 min. After being cooled on ice, the samples were clarified by centrifugation for 5 min at 14000*g*. The GlcN-Ins content was determined as described below, and the values measured after no further increase with time were used to calculate the original mycothiol *S*-conjugate concentration. For the MS−acetophenone adduct, the concentration was calculated from the absorbance at 243 nm using an ε of 13 200 (*22*).

Cloning and Expression of M. tuberculosis Rv1082. The *M. tuberculosis mca* gene (Rv1082) was amplified by PCR from genomic DNA of *M. tuberculosis* H37Rv (NCTC 7416) using the 5′-TAGCCATGGTGAGCGAACTGCGGTTGATG-3′ and 5′-GGATCCCGATCCCGGCGAACAATTCGGT-3′ primers. These primers were designed to contain an *Nco*I

restriction site at the 5′ end and a *Bam*HI site and a stop codon at the 3′ end. After denaturation for 45 s at 95 °C, 30 cycles (94 °C for 40 s, 60 °C for 1 min, and 72 °C for 1 min) were performed and the PCR product was ligated into a pCR2.1 vector (Invitrogen). Clones containing the correct size of insert inside pCR2.1 were digested with *Nco*I and *Bam*HI and separated on a 1% agarose gel. *M. tuberculosis* Rv1082 was eluted from the gel and cloned into pET16b (Novagen) that had been previously digested with *Nco*I and *Bam*HI. The ligation mix was used to transform *E. coli* DH5α. Selection of recombinants was performed on LB agar containing 100 μg/mL ampicillin. A plasmid preparation was performed from positive colonies that were found to contain the Rv1082 gene, and this preparation was used for transformation of *E. coli* BL21(DE3) from Stratagene. The transformants were selected on LB agar containing100 μg/mL ampicillin and designated PET16b Rv1082.

Enzymatic Assays. The Mca amidase activity was typically assayed by quantitation of the bimane derivative (AcCySmB) of *N*-acetylcysteine (Sigma) produced from MSmB. A representative assay contained 14 ng of enzyme in 50 μL of 50 mM HEPES (Sigma) (pH 7.5), 50 mM NaCl, and 0.1 mM dithiothreitol (Calbiochem) prewarmed to 37 °C for 1 min. The reaction was initiated by the addition of the substrate (0.1 mM MSmB). Samples (20 μL) were removed at intervals, and the reaction was quenched by mixing the sample with 60 μL of 40 mM methanesulfonic acid on ice. The mixture was centrifuged for 3 min at 14000*g* in a microcentrifuge at room temperature, and the supernatant was analyzed by shortened HPLC method 1 (*19*) to quantitate MSmB and AcCySmB.

Mca amidase activity was also assayed by assessing the production of GlcN-Ins using a minor modification of the method of Anderberg (*23*). A typical reaction included 0.1 mM mycothiol *S*-conjugate as a substrate in 100 μL of 50 mM HEPES (pH 7.5) containing 50 mM NaCl and 0.1 mM dithiothreitol at 37 °C. The reaction was initiated by addition of 14 ng of purified amidase. Samples (20 μL) were taken at 0, 3, 10, and 20 min and reactions quenched by mixing each sample with an equal volume of acetonitrile containing 10 mM NEM (Sigma) and 2 mM 1,10-phenanthroline (Kodak) followed by incubation at 60 °C for 10 min. After being cooled on ice, the samples were clarified by centrifugation for 5 min at 14000*g*. The GlcN-Ins was then derivatized with AccQ-Fluor and assayed by HPLC method 5 as previously described (*23*).

If substrates are prepared in solvents containing organic components, it is important that no significant amount of organic solvent become incorporated in the final assay since such solvents can produce substantial inhibition of Mca activity. Thus, an assay in buffer containing 5% methanol, DMSO, or acetonitrile results in a 20, 50, or 75% reduction in Mca activity with MSmB, respectively.

Purification of Mycothiol S-Conjugate Amidase. The *E. coli* pET16b Rv1082 was plated on LB agar containing 100 μg/mL ampicillin (Sigma). A single colony was taken from the plate and transferred into 50 mL of LB broth containing 100 μg/mL ampicillin. Nine 1 L cultures of LB broth containing ampicillin (100 μg/mL) were inoculated from the 50 mL culture and incubated at 37 °C with shaking. Protein expression was induced by the addition of isopropyl β-D-thiogalactopyranoside to a final concentration of 0.75 mM when the A_{600} reached 0.55, and incubation was continued overnight at 22 °C before the samples were harvested by centrifugation at 5000*g* for 20 min at 4 °C. The cells (47 g wet weight) were resuspended in 200 mL of 50 mM HEPES (pH 7.5) containing 3 mM 2-mercaptoethanol and protease inhibitors *N*-*p*-tosyl-L-phenylalanine chloromethyl ketone (Sigma) and *N*-*p*-tosyl-L-lysine chloromethyl ketone (Sigma), each at 35 μM. The cells were disrupted by sonication (Branson Sonifier Cell Disruptor 200) on ice. The extract was clarified by centrifugation for 45 min at 100000*g* at 4 °C, and the supernatant was mixed with solid ammonium sulfate to 15% saturation and incubated for 1 h on ice. After centrifugation at 15000*g* and 4 °C for 30 min, the pellet was discarded. The supernatant was adjusted to 50% saturated ammonium sulfate, incubated on ice overnight, and then centrifuged for 45 min at 15000*g* at 4 °C. The pellet was resolubilized in 120 mL of 50 mM HEPES (pH 7.5) and was desalted on a Sephadex G-25 column (Pharmacia, 7.5 cm × 36 cm). The collected eluent (250 mL) was applied at a rate of 120 mL/h to a hydroxyapatite column (Bio-gel HTP column from Bio-Rad, 2.6 cm × 38 cm), which was pre-equilibrated with 10 mM potassium phosphate buffer (pH 6.8) containing 100 mM NaCl. The bound proteins were eluted at a rate of 240 mL/h with a linear gradient from 10 to 300 mM potassium phosphate (from 100 to 0 mM NaCl) in 20 column volumes. The active fractions were pooled, and ammonium sulfate was added to 10% saturation. After 1 h on ice, the solution was clarified by centrifugation for 30 min at 10000*g* and the pellet was discarded. The supernatant was applied to a 2.6 cm × 26 cm column of Phenyl Sepharose 4B (Sigma) equilibrated with 10% saturated ammonium sulfate in 50 mM HEPES (pH 7.5) at 4 °C. The column was washed with 5 column volumes of 10% saturated ammonium sulfate and eluted with a linear gradient from 10 to 2% saturated ammonium sulfate in 50 mM HEPES (pH 7.5) over 10 column volumes. Elution was continued from 2 to 0% saturated ammonium sulfate in 50 mM HEPES (pH 7.5) over 15 column volumes, and the amidase activity eluted at 0% saturated ammonium sulfate. The active fractions were concentrated at 4 °C using a Biomax-50 (Millipore) ultrafilter. Peak activity fractions were determined by SDS−PAGE to be more than 95% pure. Protein concentrations were estimated using an extinction coefficient ϵ_{280} of 44 900 cm^{-1} M^{-1} calculated from the amino acid sequence by the method of Gill and von Hippel (*24*), verified by amino acid analysis (see below).

Inactivation by Phenanthrolines. Stock solutions (100 mM) of 1,10-phenanthroline (Kodak) and 1,7-phenanthroline (Aldrich) were prepared in 20% methanol. Solutions of Mca at 8.5 nM, 4.3 μM, and 43 μM in 50 mM HEPES (pH 7.5) with 50 mM NaCl, 0.1 mM DTT, and 1.0 mM phenanthrolines were preincubated at 37 °C for 10 min. The solutions were diluted as necessary in the same buffer to an ezyme concentration of 8.5 nM for amidase assay initiated by the addition of MSmB to a final concentration of 0.1 mM. Aliquots (20 μL) were removed at 5 and 15 min and mixed with 180 μL of 40 mM methanesulfonic acid on ice. The samples were clarified by centrifugation for 5 min at 14000*g* and injected, undiluted, onto the HPLC system for analysis using the previously described shortened HPLC method 1 (*9*).

A solution of Mca (0.43 μM) in 4 mL of 50 mM HEPES (pH 7.5) with 50 mM NaCl and 5.0 mM 1,10-phenanthroline was treated for 30 min on ice before 2 μL was removed for the amidase assay. The protein solution was then split into equal (A and B) aliquots and transferred to dialysis tubing (Spectra/Por Membrane MWCO 6-8000). All of the dialysis tubing and containers were washed with 50 mM EDTA and then rinsed with chelexed water. All buffers used for dialysis were treated over 100 mL of Chelex 100 (Sigma). Sample A was dialyzed against 600 mL of 50 mM HEPES (pH 7.5) containing 50 mM NaCl, 10 μM zinc acetate and 10 μM $CaCl_2$. Sample B was dialyzed against 600 mL of 50 mM HEPES (pH 7.5) with 50 mM NaCl with no metals. Both protein solutions were allowed to equilibrate at 4 °C for 24 h; the dialysis buffer was changed, and dialysis continued for an additional 24 h. Both samples were assayed for amidase activity as described above.

Metal Ion Content. A protein solution containing (≈0.5 mg/mL) was prepared in 50 mM HEPES (pH 7.5) with 50 mM NaCl for amino acid and metal analysis. The protein concentration of Mca (12.2 ± 0.7 μM) used for the calculation of the metal ion content was established by amino acid analysis as previously described (*18*). The metal ion content was determined by inductively coupled plasma−atomic emission spectroscopy at the Environmental Laboratory of the San Diego Gas and Electric Co. Analyses included results (milligrams per liter) for Al, Sb, As, Ba, Be, B, Cd, Ca, Cr, Co, Cu, Fe, Pb, Mg, Mn, Mo, Ni, K, Se, Si, Na, Sr, Th, Ti, V, and Zn. Results obtained with buffer alone were subtracted from those for the Mca solution to generate reported values.

Inhibition Studies. Inhibition of Mca activity by MSH with MSmB as a substrate was examined at concentrations between 1 and 20 mM MSH (*9*). The enzyme (28 ng) in 50 μL of 50 mM HEPES (pH 7.5) containing 50 mM NaCl and 0.1 mM dithiothreitol was incubated for 5 min at 37 °C prior to the start of the reaction by the addition of MSmB to a final concentration of 0.1 mM. Activity was monitored by the production of AcCySmB. Sampling and analysis for these assays are described above.

Mycothiol S-Conjugates of Rifamycin S. Stock solutions of rifamycin S (100 mM) in acetone and MSH (40 mM) in H_2O were prepared. The kinetics of the reaction of MSH (1 mM) with rifamycin S (72 μM) were studied in HEPES buffer (pH 7.5) containing 20% ethanol. An initial test reaction was monitored by wavelength scans (400−600 nm) at intervals of 3 min (Beckman DU640 spectrometer). The reaction of MSH (0.5−2.0 mM) with rifamycin S (72 μM) was then monitored at 445 nm for 30 min.

A larger-scale reaction was used for the preparation of mycothiol *S*-conjugates. A 0.5 mL reaction mixture of 4 mM rifamycin S in aqueous 50% acetonitrile with 25 mM Tris chloride (pH 8.0) was incubated with 2 mM mycothiol at 23 °C. The reaction proceeded for 3 h in the dark and was quenched by acidification to pH ~2 with 4 μL of trifluoroacetic acid. A 1 μL aliquot was diluted 100-fold for analytical HPLC analysis. Separation was carried out on a Beckman Ultrasphere IP (250 mm × 4.6 mm) analytical column equipped with a C-18 HPLC guard column using the following linear gradient: 80% A (0.05% trifluoroacetic acid in water) at 0 min, 100% B (acetonitrile) at 40 min, 20% A at 42 min, and reinjection at 60 min. The flow rate was 1 mL/min, and the effluent was monitored by absorbance at 430 nm. In addition to the rifamycin S (24.5 min), the analysis revealed two peaks at 13 min (RifS13) and 17 min (RifS17). These were isolated by preparative HPLC using the analytical method described above and taken to dryness in a Savant Speed-Vac. The samples were dissolved in H_2O at ~10 mM, and 1:100 dilutions were made in 50 mM HEPES (pH 7.5) for spectral analysis in a Beckman DU640 spectrometer for comparison with authentic rifamycin S and SV. Assignment of RifS13 as the hydroquinone form was based on the correspondence of its UV−visible λ_{max} at 445 nm with that of rifamycin SV, while RifS17 had a λ_{max} at 525 nm, identical to that of rifamycin S (*25*, *26*). Exact masses of RifS13, RifS17, rifamycin S, and rifamycin SV were assessed using MALDI-FTMS at the Scripps Research Institute Mass Spectrometry Facility (La Jolla, CA).

The concentration of RifS17 was estimated spectrophotometrically using an extinction coefficient ϵ_{525} of 4300 cm^{-1} M^{-1} for rifamycin S (*27*), and the concentration of RifS13 was similarly estimated from an extinction coefficient ϵ_{445} of 14 200 cm^{-1} M^{-1} (*28*) for rifamycin SV.

Redox Interconversion of RifS13 and RifS17. Previous studies (*25*, *26*) reported reversible reduction of rifamycin S. RifS17 (0.4 mM) in 66% methanol containing 4 mM ascorbic acid in a total volume of 80 μL was allowed to react for 30 min in the dark. A sample (20 μL) was withdrawn, diluted 1:4 in 20% acetonitrile, and analyzed by HPLC. To the remaining 60 μL was added $NaNO_2$ in 20 mM sodium acetate buffer (pH 4.6) to a final concentration of 70 mM. After 5 min, a sample was withdrawn, diluted 1:5 in 20% acetonitrile, and analyzed by HPLC.

Table 1: Purification of Recombinant *M. tuberculosis* Mca

purification step	protein (mg)	total activity (units)	specific activity (units/mg)	yield (%)	purification factor
15% SAS supernatant	4700	610	0.13	(100)	(1.00)
50% SAS pellet	3100	400	0.13	66	1.00
Sephadex G-25	3000	650	0.22	107	1.7
hydroxyapatite	430	580	1.35	95	10
Phenyl Sepharose	3.0	32	10.6	5.2	82

RESULTS

Cloning and Purification of Mca. The ORF (Rv1082) encoding the *mca* gene was cloned into the pET16b vector and expressed in *E. coli* to produce the Mca protein without a His tag. A three-step purification of the enzyme was accomplished by ammonium sulfate fractionation followed by chromatography on hydroxyapatite and then on Phenyl Sepharose (Table 1). The loss was large in the last step of purification because only fractions that were >95% pure as determined by SDS−PAGE (Figure 1A) were pooled for use in detailed studies. Other less pure fractions (Figure 1B,C) could be rechromatographed to provide additional pure product.

Metal Ion Characterization of Mca. Established methods for divalent metal ion chelation (*29*) were used to determine the importance of divalent metal ions for Mca activity. When 43 μM Mca was preincubated for 10 min with 1 mM 1,10-phenanthroline and its activity assessed in the presence of 1 mM 1,10-phenanthroline, residual activity was 0.19 ± 0.04% of that of the control (Figure 2). To determine whether this

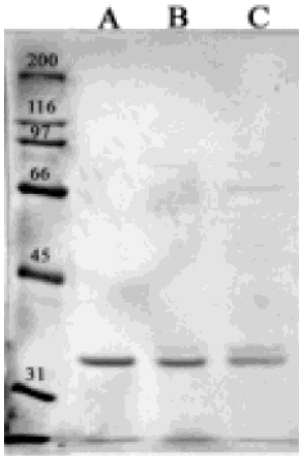

FIGURE 1: SDS−PAGE of purified recombinant Mca. Protein standards with the size in kilodaltons at the left. Mca Phenyl Sepharose fractions: (A) 215−222-pure Mca, (B) 210−214, and (C) 203−209.

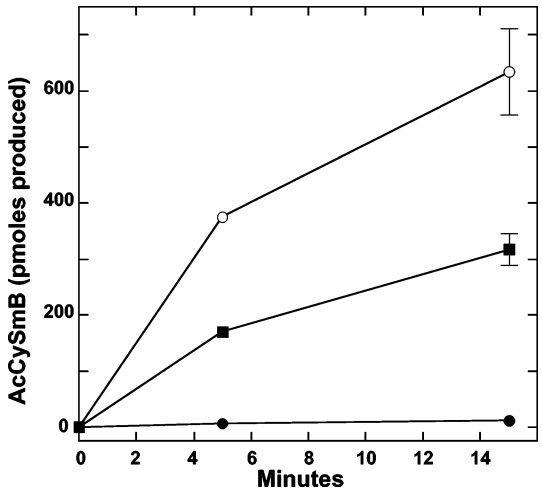

FIGURE 2: Phenanthroline inhibition of Mca activity with 0.1 mM MSmB: Mca with no phenanthroline (○), Mca with 1 mM 1,10-phenanthroline (●), and Mca with 1 mM 1,7-phenanthroline (■). Error bars are shown where the error was larger than the symbol.

inhibition is associated with the divalent metal ion chelating property of 1,10-phenanthroline or with its general aromatic character, inhibition by a nonchelating isomer was examined. Slightly more than 50% inhibition was found with 1 mM 1,7-phenanthroline (Figure 2). Thus, the 500-fold reduction in activity by 1 mM 1,10-phenanthroline is attributed primarily to its divalent metal binding capacity, suggesting that Mca requires a divalent metal ion for full activity. The experiment was repeated at 4.3 μM and 8.6 nM enzyme, and the inhibition by the phenanthrolines relative to the control was essentially the same as that at 43 μM Mca. However, at 8.6 nM Mca there was a loss (72 ± 2%) of activity of the control during the preincubation more marked than that found at the higher enzyme concentrations. When a sample of Mca was analyzed for its content of 26 different metal ions by inductively coupled plasma−atomic emission spectroscopy, it was found to contain 1.4 ± 0.1 equiv of zinc and 2.6 ± 0.2 equiv of calcium per 32 697 Da subunit.

To define conditions under which the 1,10-phenanthroline-inactivated enzyme might be reactivated, we examined the effect of zinc upon the native Mca. When Mca was assayed in the presence of varying concentrations of zinc acetate, the activity dropped significantly at concentrations above 1 μM, the activity being reduced by half at ~10 μM Zn^{2+}. This suggested that a low concentration of metal ion would need to be used in attempted regeneration studies. However, when 0.43 μM Mca was inactivated with 5 mM 1,10-phenanthroline, leaving 0.7% of the original activity, and then dialyzed at 4 °C against 50 mM HEPES (pH 7.5) containing 50 mM NaCl in the absence or presence of Zn^{2+} and Ca^{2+} (10 μM each), the activity was 0.2 or 5%, respectively, of the original activity. A non-phenanthroline-treated control dialyzed against buffer containing Zn^{2+} and Ca^{2+} retained 65% of the original activity. Thus, removal of 1,10-phenanthroline by dialysis in the presence of divalent metal ions restored activity to a level that was only ~8% of that found for Mca dialyzed without prior inactivation by 1,10-phenanthroline.

Table 2: Kinetic Parameters for Mca with Different Substrates Determined in 50 mM HEPES (pH 7.5) Containing 50 mM NaCl and 0.1 mM DTT at 37 °C with 0.28−28 ng/μL (8.6−860 nM Mca Subunit) Enzyme

amidase substrate	K_m (μM)	k_{cat} (s^{-1})	k_{cat}/K_m (M^{-1} s^{-1})
MS−MB	160 ± 40	14 ± 2	(9 ± 2) × 10^4
N-formyl-CySmB-GlcN-Ins	620 ± 70	2.6 ± 0.2	(4.2 ± 0.6) × 10^3
CySmB-GlcN-Ins	−	−	100 ± 10[a]
GlcNAc-Ins	>2000	>6 × 10^{-4}	0.30 ± 0.01[a]
AcCySmB-GlcN[b]	−	−	1.2 ± 0.1[a]
MSSM	4800 ± 1300	1.7 ± 0.7	350 ± 170
MS−acetophenone	690 ± 50	37 ± 2	(5.4 ± 0.5) × 10^4
MS−cerulenin	650 ± 130	7 ± 1	(1.1 ± 0.3) × 10^4
MS−CPM	440 ± 90	1.3 ± 0.2	(3.0 ± 0.8) × 10^3
MS−MPB	>3000	>3	(1.03 ± 0.02) × 10^3 [a]
MS−ME	1300 ± 300	15 ± 2	(1.2 ± 0.3) × 10^4
RifS13	190 ± 30	0.82 ± 0.08	(4.3 ± 0.8) × 10^3
RifS17	450 ± 80	1.04 ± 0.12	(2.3 ± 0.5) × 10^3

[a] No saturation detected and value determined from the slope of rate vs substrate concentration. Limits for K_m and k_{cat} are given on the basis of the maximum substrate concentration tested if above 1 mM. [b] Reaction assayed for the production of AcCyS-mB.

Enzyme Kinetics and Substrate Specificity. A variety of substrates were examined using the purified Mca at 37 °C in 50 mM HEPES (pH 7.5) containing 50 mM NaCl and 0.1 mM DTT. Values of K_m and k_{cat} (M_r = 32 697 Da) were determined from Eadie−Hofstee plots, and the results are presented in Table 2. In some cases, saturation was not detected because of a very high K_m value or because of the limited availability of the substrate, and the value of k_{cat}/K_M was assessed from the slope of the increase of V with substrate concentration.

The pattern of reactivity for *M. tuberculosis* Mca (Table 2) is generally similar to that reported earlier for *M. smegmatis* Mca (*9*). However, the specific activities for the *M. tuberculosis* Mca with MSmB as a substrate (Table 1) are roughly 3-fold higher than the previously published values for the *M. smegmatis* Mca. This general increase in the rates can largely be attributed to the more optimal assay buffer conditions used here. The earlier assays were conducted at a low ionic strength and temperature [25 mM HEPES (pH 7.5) and 30 °C, respectively], whereas the assays described here used a higher ionic strength and temperature [50 mM HEPES (pH 7.5) and 50 mM NaCl and 37 °C, respectively] as employed for other metalloproteins (*30*). When *M. tuberculosis* Mca was assayed under the previously published conditions, the following values were obtained with

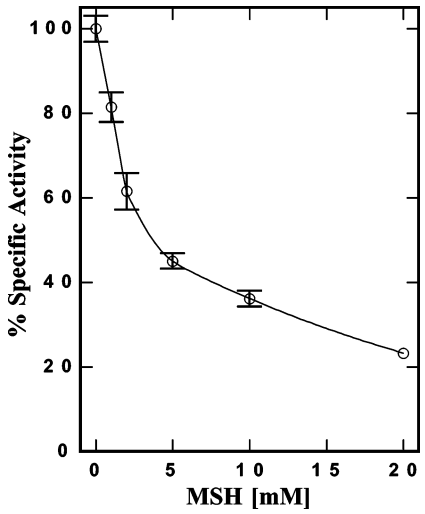

FIGURE 3: Inhibition of Mca activity with 0.1 mM MSmB by MSH. Error bars are shown where the error was larger than the symbol.

MSmB as a substrate: $K_m = 460 \pm 60$ μM, $k_{cat} = 14.5 \pm 1.4$ s^{-1}, and $k_{cat}/K_m = (3.2 \pm 0.5) \times 10^4$ M^{-1} s^{-1}. The latter value is slightly less than half that [$k_{cat}/K_m = (8.4 \pm 1.3) \times 10^4$ M^{-1} s^{-1}] calculated from the parameters reported for *M. smegmatis* Mca (*9*). These parameters were not available for MSH which gave more complex kinetics with *M. tuberculosis* Mca (see below), but the activity of MSH at 0.1 mM under the earlier assay conditions was ~75% higher than that published for *M. smegmatis* Mca (*9*).

The results in Table 2 and Figure 4 show that the integrity of the mycothiol moiety is an important factor in determining substrate activity, as will be described in detail in Discussion. Although Mca is relatively specific for the mycothiol moiety of mycothiol *S*-conjugates, it is more flexible in its requirements with respect to the *S*-conjugate moiety. The best substrate tested thus far is MSmB, which is approximately twice as reactive as the MS−acetophenone adduct. The MS−cerulenin and MS−ME adducts have similar reactivities, ~10% of that of MSmB, whereas the MS−CPM and MS−MPB adducts are substantially less reactive.

The least reactive substrate of Table 2 is GlcNAc-Ins and is of special interest because of its role in MSH biosynthesis. A homologue of Mca, the deacetylase MshB, has a high activity with GlcNAc-Ins and a lower activity toward MSmB (*20*). It plays a key roll in MSH biosynthesis by conversion of GlcNAc-Ins to GlcN-Ins which is then ligated with cysteine and acetylated by acetylCoA to produce MSH (*4*). A null mutant in *mshB* has been produced in *M. tuberculosis* and accumulates large amounts of GlcNAc-Ins but still produces MSH, albeit at a slower rate (*31*). Thus, some other enzyme has a weak ability to catalyze the deacetylation of GlcNAc-Ins, and Mca appeared to be a logical candidate. We therefore evaluated the GlcNAc-Ins deacetylase activity of Mca. The activity of Mca was measured at GlcNAc-Ins concentrations from 0.05 to 2 mM and found to increase linearly with no evidence of saturation. Least-squares analysis of the data demonstrated that the dependence upon GlcNAc-Ins had a slope of 0.55 ± 0.02 nmol min^{-1} mg^{-1} (mM GlcNAc-Ins)$^{-1}$, from which the k_{cat}/K_M value was calculated (Table 2). Detailed calculations using this value to estimate the activity under cellular conditions gave a value that was sufficient to account for the production of MSH by the *M. tuberculosis mshB* null mutant (*31*).

MSH as a Substrate and Inhibitor of Mca. Since MSH is present at high concentrations in mycobacteria, we examined its role as a substrate and as an inhibitor for Mca. The cleavage of MSH by Mca measured over the concentration range of 0.1−10 mM did not follow simple Michaelis−Menten kinetics, a plot of *V* versus MSH concentration being sigmoidal. A V_{max} value of 800 ± 100 nmol min^{-1} mg^{-1} was estimated by extrapolation of the reciprocal values of the rates at the highest MSH concentration to infinite concentration and utilized to construct a Hill plot. The slope of the latter yielded a Hill coefficient n_H of 1.28 ± 0.05. Rates determined at 2 and 5 mM MSH, representing physiologic concentrations for *M. smegmatis* and *M. tuberculosis*, respectively, were 190 ± 30 and 290 ± 10 nmol min^{-1} mg^{-1}, respectively, and provide a basis for estimating the extent of MSH degradation resulting from the action of Mca.

To test whether MSH inhibits the amidase activity of Mca toward mycothiol *S*-conjugates under physiologic conditions, we examined the Mca amidase activity with 0.1 mM MSmB

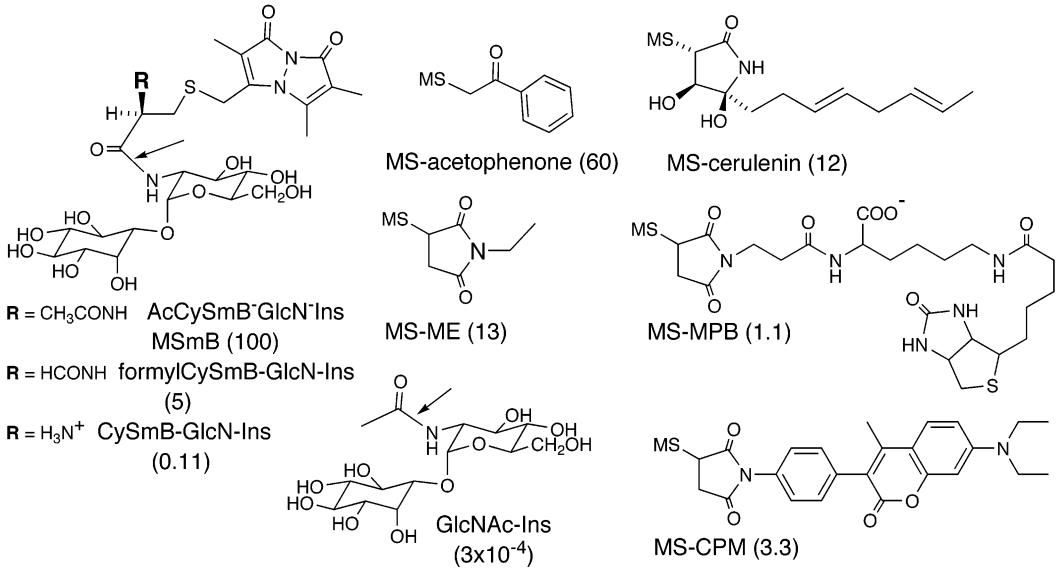

FIGURE 4: Structures for selected Mca substrates. Values in parentheses are rates relative to that for MSmB calculated from the k_{cat}/K_m values of Table 2. Arrows denote the amide bond cleaved by Mca.

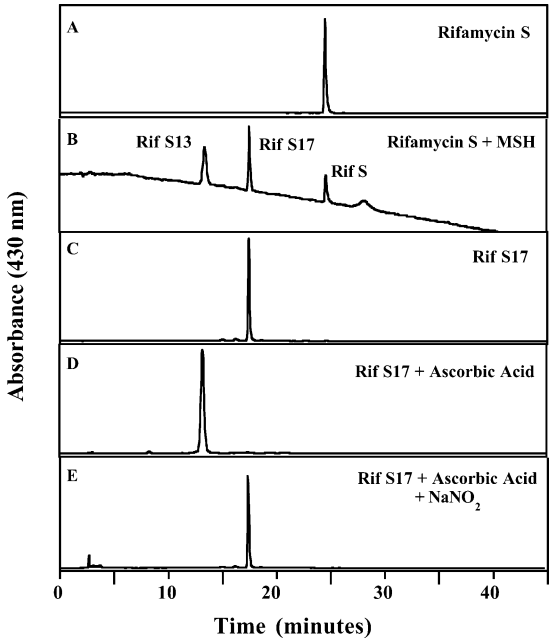

FIGURE 5: Reverse phase HPLC analysis of the reaction of mycothiol with rifamycin S and interconversion of mycothiol *S*-conjugates of rifamycin S: (A) pure rifamycin S, (B) 2 equiv of rifamycin S reacted with 1 equiv of MSH at room temperature for 3 h, (C) HPLC-purified RifS17, (D) RifS17 reacted with excess ascorbic acid, and (E) RifS17 reacted with ascorbic acid followed by reaction with excess $NaNO_2$.

as a substrate in the presence of millimolar levels of MSH (Figure 3). The amidase activity was monitored by production of AcCySmB and was not impacted by the production of AcCys from hydrolysis of MSH which even at 20 mM MSH proceeded at ~10% of the rate of MSmB hydrolysis. Mca was 50% inhibited at 3 mM MSH and at 20 mM MSH Mca still retained 23% of its original activity. This indicates that MSH at a concentration of >3 mM may produce some inhibition of Mca, but even at high levels of MSH, Mca still retains significant activity.

Production of Mycothiol Conjugates of Rifamycin S and Their Assessment as Substrates for Mca. Since MSH-deficient mutants are more sensitive to rifampin than the parent strain, it seemed possible that MSH is involved in antibiotic detoxification (*10*, *11*). The native antibiotic rifamycin S is known to react with thiols (*26*), so it seemed likely that MSH would form a conjugate with it. When rifamycin S was reacted with mycothiol under physiologically relevant conditions (Figure 5A), the reaction produced two highly colored products chromatographically distinguishable from the parent compound (Figure 5B). The two new compounds were designated RifS13 and RifS17 according to their elution times. RifS13 and RifS17 were purified by HPLC, and an exact mass was obtained for each compound by MALDI-FTMS. The results, 1204.49 Da (RifS13) and 1204.44 Da (RifS17), both correspond to the mass of MSH bound to a sodium salt of rifamycin SV. A major fragmentation product present in both RifS17 and RifS13 samples at *m*/*e* 718 [M − MSH (486 Da)] peak corresponds to the loss of the mycothiol moiety from the rifamycin SV molecule. As controls, the exact masses for the sodium salt forms of both rifamycin S and rifamycin SV were determined to be 720.30 and 720.29 Da, respectively. A major fragmentation product at M − 32 Da was

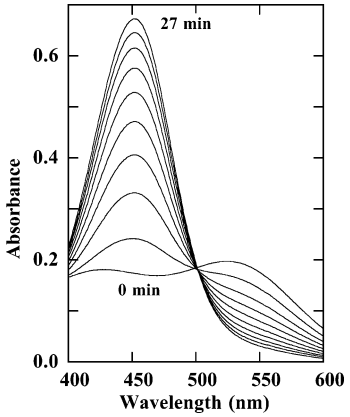

FIGURE 6: Spectral monitoring (400−600 nm) of the reaction of rifamycin S (72 μM) and MSH (1 mM) taken at 3 min intervals from 0 (prior to MSH addition) to 27 min.

observed for all samples. This fragment is reportedly generated by the loss of the C-27 hydroxymethyl from rifamycin (*32*).

The reaction of MSH with rifamycin S was followed kinetically by UV−visible spectroscopy (Figure 5). The weak absorption of rifamycin S with a λ_{max} of 525 nm is replaced by the stronger absorption with a λ_{max} of 445 nm characteristic of rifamycin SV. This verifies that RifS13 is the initial reaction product (Figure 6) and suggests that RifS17 is formed by a subsequent air oxidation. The phenomenon of reversible oxidation and reduction interconverting the hydroquinone and quinone forms is well-established (*25*, *26*). HPLC was used to monitor the reaction of the RifS17 (Figure 5C) with ascorbic acid to produce a retention time corresponding to the hydroquinone RifS13 (Figure 5D). With the addition of the oxidizing agent $NaNO_2$, the reaction was reversed to produce the quinone form RifS17 (Figure 5E). These reactions are shown in Figure 7.

The kinetics of the reaction of MSH (0.5−2.0 mM) with rifamycin S (72 μM) were studied in HEPES buffer (pH 8) at 23 °C. The reaction was shown to follow second-order kinetics, first-order in each reactant, with a k_2 of $(1.1 \pm 0.1) \times 10^{-6}$ M^{-1} s^{-1}.

HPLC-purified RifS13 and RifS17 were utilized as substrates for Mca, and the amidase product GlcN-Ins was assayed by HPLC. The results (Table 2) show that these are fair substrates for Mca, 20−40-fold less reactive than MSmB.

DISCUSSION

The specific activities for Mca of *M. tuberculosis* and *M. smegmatis* are roughly comparable when tested with MSmB and MSH as substrates under the same assay conditions. The pattern of substrate specificity of the *M. tuberculosis* enzyme (Table 2) is qualitatively similar to that reported for *M. smegmatis* Mca, although detailed kinetic analysis was not performed in the latter case (*9*). Also, inhibition of Mca activity with MSmB by MSH was similar for the two enzymes (*9*). Thus, the properties of the *M. tuberculosis* and *M. smegmatis* enzymes are similar, as might be expected from their high degree of sequence identity.

The amino acid sequence of *M. tuberculosis* Mca is 72% identical to that of the *M. smegmatis* enzyme (Figure 8). Comparable or higher levels of sequence identity are found for sequences of Mca orthologs from other mycobacteria,

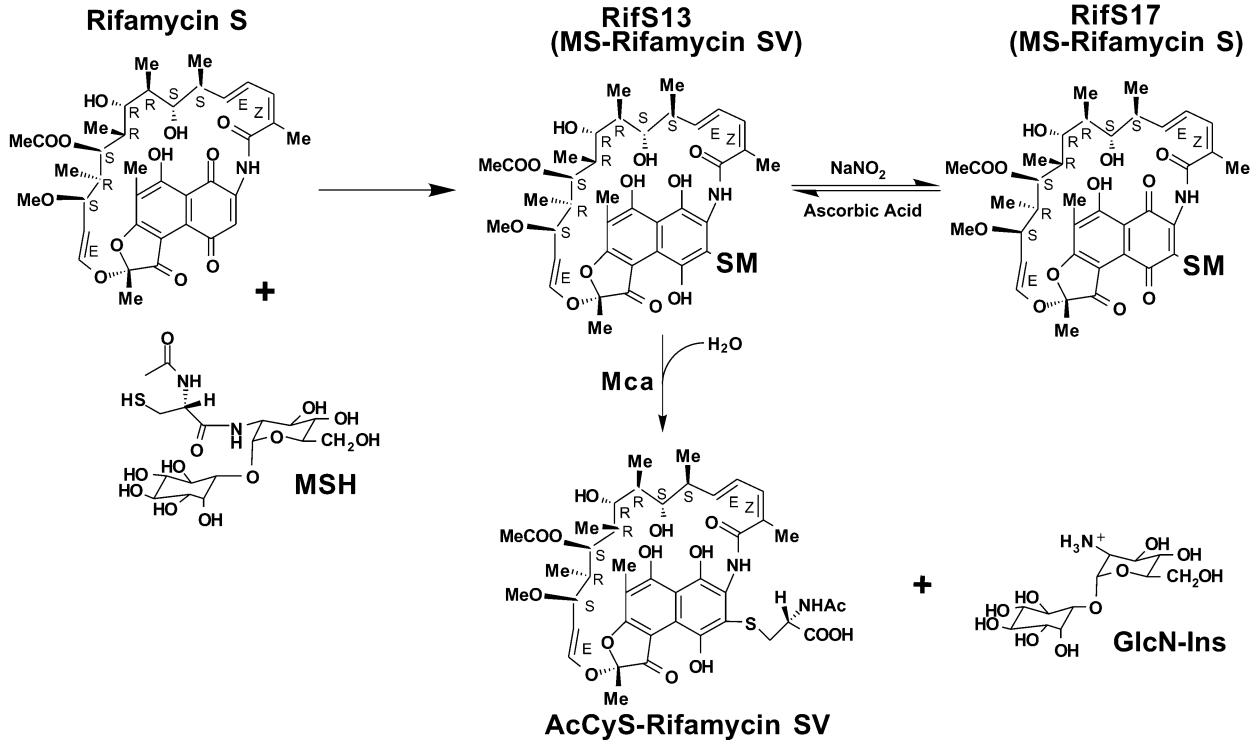

FIGURE 7: Scheme for the reaction of MSH with rifamycin S to produce RifS13, the reversible oxidation of RifS13 to RifS17, and the hydrolysis of RifS13 catalyzed by Mca.

```
                     1                                                               65
Mca M. tuberc.    1 MSE-LRLMAVHAHPDDESSKGAATLARYADEGHRVLVVTLTGGERGEILNPAMD--LPDVHGRIA
Mca M. smegmat.   1 MSE-LRLMAVHAHPDDESSKGAATTARYAAEGARVMVVTLTGGERGDILNPAMD--LPEVHGRIA
Mca C. glutam.    1 MSG-LRLMAIHAHPDDESSKGAATMARYAAEGNQVMVVTCTGGERGDILNPAMD--KPGILDNIF
Mca T. fusca      1 -------MAVHAHPDDESSKGAATMARYVNEGAEVLVVTLTGGERGSILNPAMD--RPEIRENIA
Mca S. coelic.    1 MTDQLRLMAVHAHPDDESSKGAATMAKYVSEGVDVLVVTCTGGERGSILNPKLQG-DAYIEENIH
MshB M. tuberc.   1 MSETPRLLFVHAHPDDESLSNGATIAHYTSRGAQVHVVTCTLGEEGEVIGDRWAQLTADHADQLG
                    66                                                              130
Mca M. tuberc.   63 EIRRDEMTKAAEILGV-EHTWLGFVDSGLPKGDLPP-PLPDDCFARVPLEVSTEALVRVVREFRP
Mca M. smegmat.  63 EVRRDEMAKAAEILGV-EHHWLGFVDSGLPEGDPLP-PLPDGCFALVPLEEPVKRLVRVIREFRP
Mca C. glutam.   63 AVRQEEMAKAMEILGT-EHRWLGYEDSGLPQGDPLP-PLPEGCFALEDSDKVTQDLVKILREFRP
Mca T. fusca     57 EVRRKEMEEARRILGV-RQVFVGFIDSGLPEGDPPP-PLPEGCFALQPLEVAAEPVVRLVREFRP
Mca S. coelic.   65 EVRRKEMDEAREILGV-GQEWLGFVDSGLPEGDPLP-PLPEGCFALEDVDKAAGELVRKIRSFRP
MshB M. tuberc.  66 GYRIGELTAALRALGVSAPIYLGGAGRWRDSGMAGTDQRSQRRFVDADPRQTVGALVAIIRELRP
                    131                                                             195
Mca M. tuberc.  126 HVMTTYDENGGYPHPDHIRCHQVSVAAYEAAGDFCRFPDA--GEPWTVSKLYYVHGFLRERMQML
Mca M. smegmat. 126 HVMTTYDENGGYPHPDHIRCHQVSVAAYEAAADHLLYPDA--GEPWAVQKLYYNHGFLRQRMQLL
Mca C. glutam.  126 HVIITYDENGGYPHPDHLKVHEVSMLAWEKSGDAAYAPEL--GAPWEPLKLYYTHGFIRQRMEMF
Mca T. fusca    120 HVMITYDEQGGYPHPDHIMCHKVSVEAFEAAADPERYPGT--GEPWQTSKLYYHVSFPLERFEAI
Mca S. coelic.  128 QVITTYDENGGYPHPDHIMTHKITMVAFEGAADTEKYPESEYGTAYQPLKVYYNQGFNRPRTEAL
MshB M. tuberc. 131 HVVVTYDPNGGYGHPDHVHTHTVTTAAVAAGVGSGTADHP-GDPWTVPKFYWTVLGLSALISGA
                    196                                                             260
Mca M. tuberc.  189 QDEFARHGQRGPFEQWLAYWDPDHDFLTSRVTTRVECSKYFSQRDDALRAHATQI--DPNAEFFA
Mca M. smegmat. 189 QEEFAKNGQEGPFAKWLEHWDPDNDVFANRVTTRVHCAEYFHQRDDALRAHATQI--DPKGDFFH
Mca C. glutam.  189 HDLLIEQGKPSPYTPMLERWKANEADVMARVTTQVPCERFFDQRDDALRAHATQI--DPAGAFFG
Mca T. fusca    183 AKVLSDRGMENPYADWMKRLE-KRDTRRWEITTRVECGEYFEVRDRALLAHATQI--DPNSFWFA
Mca S. coelic.  193 HHALLDRGLESPYEDWLKRWS-EFERKERTLTTHVPCADFFEIRDKALIAHATQI--DPEGGWFR
MshB M. tuberc. 195 RALVPDDLRPEWVLPRADEIAFGYSDDGIDAVVEADEQAR-AAKVAALAAHATQVVVGPTGRAAA
                    261                                     305
Mca M. tuberc.  252 APLAWQERLWPTEEFELARSRIPARPP---ETELFAGIEP-----
Mca M. smegmat. 252 APIEWQQRLWPTEEFELARARVPVTLP---EDDLFKGVEP-----
Mca C. glutam.  252 TPVEVQRRLWPTEEFELAKTRVKTSIP---EDDLFAGITPDAE--
Mca T. fusca    245 VPNDIQREAWPTEDYHLARSFVDTELP---EDDLFAGIRDKV---
Mca S. coelic.  255 VPMEIQKEVWPTEEYELAKSLVETSLP---EDDLFAGIRDNA---
MshB M. tuberc. 259 LSNNLALPILADEHYVLAGGSAGARDERGWETDLLAGLGFTASGT
```

FIGURE 8: Sequence alignment (GenBank entries) for Mca from *M. tuberculosis* (NP_215598), *C. glutamicum* (NP_600215), *T. fusca* (ZP_00057450), and *S. coelicolor* (NP_629119) and for MshB (Rv1170) from *M. tuberculosis* (NP_215686).

including *Mycobacterium bovis*, *Mycobacterium leprae*, and *Mycobacterium avium*. Orthologs of the *M. tuberculosis* Mca are also found in *Corynebacterium glutamicum* (59% identical), *Thermobifida fusca* (36% identical), and *Streptomyces coelicolor* A3(2) (52% identical), and their sequences are shown in Figure 8. Also included is the sequence of *M. tuberculosis* MshB (Rv1170), a closely related homologue (42% identical) which catalyzes deacetylation of GlcNAc-

Ins but also has amidase activity with mycothiol *S*-conjugates (*9*). The similarity between these structures extends throughout the entire sequence, although for MshB the resemblance is greatest in the N-terminal half of the chain. Although MshB exhibits amidase activity toward mycothiol *S*-conjugates, its primary amidase activity is the deacetylation of GlcNAc-Ins, a key step in mycothiol biosynthesis, and it is therefore termed the "deacetylase" (*20*, *31*, *34*). For Mca, on the other hand, the deacetylation of GlcNAc-Ins is significantly slower than the amidase activity with even the least reactive mycothiol *S*-conjugates (Table 2).

Mca is dependent upon divalent metal ions for activity, and the pure enzyme contains Zn^{2+} and Ca^{2+} as the only divalent metals. Since Zn^{2+}, but not Ca^{2+}, is a common catalytic component in amidases, this strongly suggests that Mca is a zinc metalloenzyme. Since Mca and MshB are closely related, MshB is presumably also a zinc metalloprotein. There are a large number of residues with side chains that can serve as potential ligands for Zn^{2+} and are conserved among all of the sequences shown in Figure 8. These include Asp14, -15, -132, and -141, Glu16, -44, -68, -264, and -279, and His10, -12, -139, -142, -146, and -239 as numbered in the *M. tuberculosis* Mca sequence. Identification of those actually involved in metal binding will have to await the results of X-ray crystallographic studies.

The results presented here allow a refinement of the insights gained from earlier studies of *M. smegmatis* Mca concerning the substrate specificity of the enzyme. With respect to the mycothiol portion of the mycothiol *S*-conjugate, the activity is strongly dependent upon the structure of the AcCys moiety. Removal of the methyl residue of the acetyl group of MSmB (Figure 4) to produce *N*-formyl-CySmB-GlcN-Ins leads to a 20-fold loss of activity, whereas complete removal of the acetyl group to produce CySmB-GlcN-Ins, with the cysteinyl amino group now presumably charged at neutral pH, results in a nearly 10^3-fold drop in activity. If the Cys residue is removed completely, leaving GlcNAc-Ins, the activity falls by a factor of 3×10^5. Removal of the Ins residue at the other end of the mycothiol molecule to produce AcCySmB-GlcN results in an 8×10^4-fold reduction in activity (Table 2). Although Mca appears to be quite specific with regard to the components of MSH, it was recently reported that substitution of the Ins group of MSmB with a cyclohexane mercaptan moiety to generate a thioglycoside resulted in an only 2-fold drop in activity with Mca (*35*). Thus, the Ins residue can apparently be substituted with other cyclohexane derivatives without a major loss of activity. Cys-GlcN-Ins and AcCys-GlcN are not found at significant levels in mycobacteria (*23*), so it is unlikely that their *S*-conjugates play any role *in vivo*.

Mca is more accepting of changes in the *S*-conjugate group of the substrate and will tolerate groups of widely varying structure (Table 2 and Figure 4). Replacement of the ethyl group at the maleimide residue of the MS−ME adduct with the bulkier groups present in the MS−MPB and MS−CPM adducts (Figure 4) reduces activity but does not eliminate it. The MSH conjugate of cerulenin, an antibiotic active against mycobacteria (*36*), is somewhat similar to the MS−ME conjugate but contains two hydroxyl groups in the five-membered ring and a longer hydrocarbon chain; it has reactivity comparable to that of the MS−ME conjugate. Only the MS−acetophenone adduct approximated MSmB in reactivity, being 60% as reactive, but with rather different and compensating K_m and k_{cat} values (Table 2). The results suggest that there is a hydrophobic pocket in Mca which can accommodate the bimane or acetophenone group. The intervening methylene group in both conjugates may provide flexibility in optimizing the fit of the rings.

The acetophenone moiety (Figure 4) is substantially similar in structure to the prodrug isoniazid. This suggests that an MSH adduct or derivative of isoniazid would likely be a good substrate for Mca. However, it is not at all clear what adduct would be formed or what role the cleavage might play in the currently proposed processes for activation of isoniazid (*37*).

GlcNAc-Ins is found at low levels (~1 nmol/10^9 cells or ~0.2 mM) in exponential cells of *M. tuberculosis* (*31*). In a *M. tuberculosis mshB* null mutant, the GlcNAc-Ins level was found to be much higher, increasing from 5 to ~30 mM upon the transition from the exponential to stationary phase (*31*). This accumulation of GlcNAc-Ins was expected due to inactivation of MshB, the GlcNAc-Ins deacetylase involved in MSH biosynthesis (*20*). Surprisingly, a low level of MSH was still produced, and this increased to above normal levels in the stationary phase (*31*). Another enzyme was apparently substituting for MshB and deacetylating GlcNAc-Ins at a slow rate. In fact, the low but measurable rate of deacetylation of GlcNAc-Ins by *M. tuberculosis* Mca as determined here proved to be of the correct magnitude to account for the observed production of MSH (*31*). At the concentration of GlcNAc-Ins of ~5 mM measured for exponential cells of the *M. tuberculosis* Erdman *mshB* null mutant, the production of GlcN-Ins was estimated to be ~1 nmol day^{-1} $(10^9 \text{ cells})^{-1}$ or ~3 nmol/10^9 cells for each cell division. Thus, if Mca were the source of MSH in the *mshB* null mutant, one would predict that its MSH content during exponential growth would drop from the normal value of 10 nmol/10^9 cells to ~3 nmol/10^9 cells which agrees well with the observed value of 2−3 nmol/10^9 cells (*31*).

The finding that MSH is itself a weak substrate for Mca raises the possibility of a degradative pathway in which Mca cleaves MSH to produce AcCys and GlcN-Ins. The AcCys might be lost from the cell or be hydrolyzed to release cysteine (*23*). The cysteine and the GlcN-Ins would then be ligated via the action of MshC (*38*), and mycothiol would be resynthesized from the product via the action of mycothiol synthase, MshD (*19*). On the basis of the activity at 3 mM MSH and if it is assumed that 0.04% of the total cellular protein is Mca, as found for *M. smegmatis* (*9*), it can be estimated that the degradation of MSH would occur at a rate of ~20% per hour. This may represent a tolerable side effect of the beneficial degradation of mycothiol *S*-conjugates by Mca, or it may have some favorable consequence for the cell that is not yet apparent. Alternatively, the activity determined with the purified protein in dilute solution may not accurately reflect the environment in the cell where self-aggregation or association with other cellular components could produce changes in Mca, resulting in a decreased level of MSH hydrolysis.

The largest mycothiol *S*-conjugates that were tested are those produced from rifamycin S, and these proved to have modest activity with Mca. The rifamycin adducts represent the most complex mycothiol *S*-conjugates that have been studied (Figure 7), and it might have been expected that the

complexity of the structure would result in rather minimal activity with Mca. However, the k_{cat}/K_m values are 3−5% of that for MSmB which might very well be sufficient for Mca to play a role in the detoxification of rifamycin S in cells. To address this issue, studies of the metabolism of rifamycin S by *M. smegmatis* are being carried out.

In summary, the results presented here demonstrate that *M. tuberculosis* Mca is very similar to *M. smegmatis* Mca and that it is active with a wide variety of mycothiol *S*-conjugate substrates in which the *S*-conjugate group is variable but the mycothiol moiety must be substantially intact. Mca is a zinc metalloprotein in which the metal ion is associated with the activity. The enzyme has a low deacetylase activity with GlcNAc-Ins, but the rate is sufficient to account for the slow production of MSH observed in an *M. tuberculosis* mutant deficient in the normal deacetylase, MshB. Rifamycin S readily reacts with MSH to form an *S*-conjugate under physiologic conditions; this *S*-conjugate, and its oxidized form, are modest substrates for Mca. These results provide a basis for the rational design of inhibitors of Mca and of experiments for testing the cellular detoxification of rifamycin S by MSH.

ACKNOWLEDGMENT

We thank Rakesh M. Vohra for his generous gift of the rifamycin S and Mary Ko for expert technical assistance. R.C.F. and Y.A. were consultants for Exegenics Inc. during the initial phase of these studies.

REFERENCES

1. Newton, G. L., Arnold, K., Price, M. S., Sherrill, C., delCardayré, S. B., Aharonowitz, Y., Cohen, G., Davies, J., Fahey, R. C., and Davis, C. (1996) *J. Bacteriol. 178*, 1990−1995.
2. Patel, M. P., and Blanchard, J. S. (1999) *Biochemistry 38*, 11827−11833.
3. Patel, M. P., and Blanchard, J. S. (2001) *Biochemistry 40*, 3119−3126.
4. Newton, G. L., and Fahey, R. C. (2002) *Arch. Microbiol. 178*, 388−394.
5. Norin, A., Van Ophem, P. W., Piersma, S. R., Persson, B., Duine, J. A., and Jornvall, H. (1997) *Eur. J. Biochem. 248*, 282−289.
6. Misset-Smits, M., van Ophem, P. W., Sakuda, S., and Duine, J. A. (1997) *FEBS Lett. 409*, 221−222.
7. Duine, J. A. (1999) *Biofactors 10*, 201−206.
8. Vogt, R. N., Steenkamp, D. J., Zheng, R., and Blanchard, J. S. (2003) *Biochem. J. 374*, 657−666.
9. Newton, G. L., Av-Gay, Y., and Fahey, R. C. (2000) *Biochemistry 39*, 10739−10746.
10. Newton, G. L., Unson, M. D., Anderberg, S. J., Aguilera, J. A., Oh, N. N., delCardayré, S. B., Davies, J., Av-Gay, Y., and Fahey, R. C. (1999) *Biochem. Biophys. Res. Commun. 255*, 239−244.
11. Rawat, M., Newton, G. L., Ko, M., Martinez, G. J., Fahey, R. C., and Av-Gay, Y. (2002) *Antimicrob. Agents Chemother. 46*, 3348−3355.
12. Stevens, J. L., and Jones, D. P. (1989) in *Glutathione: Chemical, Biochemical, and Medical Aspects, Part B* (Dolphin, D., Poulson, R., and Avramovic, O., Eds.) pp 45−84, John Wiley, New York.
13. Nicholas, G. M., Newton, G. L., Fahey, R. C., and Bewley, C. A. (2001) *Org. Lett. 3*, 1543−1545.
14. Nicholas, G. M., Eckman, L. L., Ray, S., Hughes, R. O., Pfefferkorn, J. A., Barluenga, S., Nicolaou, K. C., and Bewley, C. A. (2002) *Bioorg. Med. Chem. Lett. 12*, 2487−2490.
15. Nicholas, G. M., Eckman, L. L., Newton, G. L., Fahey, R. C., Ray, S., and Bewley, C. A. (2003) *Bioorg. Med. Chem. 11*, 601−608.
16. Habeck, M. (2002) *Targets 1*, 53−54.
17. Unson, M. D., Newton, G. L., Davis, C., and Fahey, R. C. (1998) *J. Immunol. Methods 214*, 29−39.
18. Newton, G. L., Fahey, R. C., Cohen, G., and Aharonowitz, Y. (1993) *J. Bacteriol. 175*, 2734−2742.
19. Koledin, T., Newton, G. L., and Fahey, R. C. (2002) *Arch. Microbiol. 178*, 331−337.
20. Newton, G. L., Av-Gay, Y., and Fahey, R. C. (2000) *J. Bacteriol. 182*, 6958−6963.
21. Fahey, R. C., and Newton, G. L. (1987) *Methods Enzymol. 143*, 85−96.
22. Braude, E. A., and Sondheimer, F. (1955) *J. Chem. Soc.*, 3754−3766.
23. Anderberg, S., Newton, G. L., and Fahey, R. C. (1998) *J. Biol. Chem. 273*, 30391−30397.
24. Gill, S. C., and von Hippel, P. H. (1989) *Anal. Biochem. 189*, 319−326.
25. Pasqualucci, C. R., Vigevani, A., Radaelli, P., and Gallo, G. G. (1970) *J. Pharm. Sci. 59*, 685−687.
26. Dampier, M. F., Chen, C. W., and Whitlock, H. W., Jr. (1976) *J. Am. Chem. Soc. 98*, 7064−7069.
27. Oppolzer, W., Prelog, V., and Sensi, P. (1964) *Experientia 20*, 336−339.
28. Bergamini, N., and Fowst, G. (1965) *Arzneim.-Forsch. 15* (Suppl.), 951−1002.
29. Wagner, F. W. (1988) *Methods Enzymol. 158*, 21−31.
30. Jackman, J. E., Raetz, C. R. H., and Fierke, C. A. (2001) *Biochemistry 40*, 514−523.
31. Buchmeier, N., Newton, G. L., Koledin, T., and Fahey, R. C. (2003) *Mol. Microbiol. 47*, 1723−1732.
32. Zerilli, L. F. L., Gallo, G. G., Maurer, K. H., and Rapp, U. (1975) *Biomed. Mass Spectrom. 2*, 307−312.
33. Newton, G. L., Koledin, T., Gorovitz, B., Rawat, M., Fahey, R. C., and Av-Gay, Y. (2003) *J. Bacteriol. 185*, 3476−3479.
34. Rawat, M., Kovacevic, S., Billman-Jacobe, H., and Av-Gay, Y. (2003) *Microbiology 149*, 1341−1349.
35. Knapp, S., Gonzalez, S., Myers, D. S., Eckman, L. L., and Bewley, C. A. (2002) *Org. Lett. 4*, 4337−4339.
36. Rastogi, N., Goh, K. S., Horgen, L., and Barrow, W. W. (1998) *FEMS Immunol. Med. Microbiol. 21*, 149−157.
37. Rozwarski, D. A., Grant, G. A., Barton, D. H., Jacobs, W. R., Jr., and Sacchettini, J. C. (1998) *Science 279*, 98−102.
38. Sareen, D., Steffek, M., Newton, G. L., and Fahey, R. C. (2002) *Biochemistry 41*, 6885−6890.

BI030080U